Rare Met. (2014) 33(2):191–195
DOI 10.1007/s12598-013-0149-3

RARE METALS
www.editorialmanager.com/rmet

Microstructure and properties of Al_2O_3 dispersion-strengthened copper fabricated by reactive synthesis process

Xue-Hui Zhang, Chen-Guang Lin*,
Shun Cui, Zeng-De Li

Received: 26 October 2012 / Revised: 18 March 2013 / Accepted: 10 April 2013 / Published online: 24 October 2013

Abstract Al_2O_3 dispersion-strengthened copper alloy was prepared by reactive synthesis and spark plasma sintering (SPS) process. Studies show that nano-sized γ-Al_2O_3 particles with 27.4 nm mean size and 50-nm interval are homogeneously distributed in copper matrix. The density of SPS alloy is about 99 %, meanwhile, the electrical conductivity of sintered alloy is 72 % IACS and the Rockwell hardness can reach to HRB 91.

Keywords Dispersion-strengthened copper; Reactive synthesis; Spark plasma sintering

1 Introduction

Al_2O_3 dispersion-strengthened copper (DSC) alloy is a family of composite materials by using Al_2O_3 nanoscale particles as strengthening phase and finely dispersed in the copper matrix [1, 2], which has the properties of high strength, high electrical conductivity at room temperature, and excellent high temperature characteristics (HTC). As a result, it is widely used as a variety of electrical conductors and heat conductors where such as large scale integrated circuit lead frames, resistance welding electrode, high speed railway over-head conductors, and microwave communication jamming system are required [3, 4]. At present, Al_2O_3 DSC alloy can be produced by various processing methods [5, 6] such as internal oxidation [7], co-precipitation, sol–gel, mechanical alloying [8], reactive spray deposition [9], reaction milling [10, 11], etc. Internal oxidation process can obtain uniformly distributed Al_2O_3 nano-sized particles by means of in situ formation, so the method is now the most successful technique for industrialized production of high performance Al_2O_3 DSC alloys. However, the traditional internal oxidation process always uses solid-phase (Cu_2O) and gaseous-phase (purity nitrogen mix with oxygen) as oxygen source to selective oxidation at selected temperature in a gas shielded or sealed container. The method has some shortcomings which needed to be improved, for example, the process is so complicated that the quality of the alloys is not easy to control and the cost is too high to be applied widely in industry.

In recent years, a novel reactive synthesis (RS) process to fabricate Al_2O_3 DSC alloy with high quality has been exploring in our department. In this paper, the effects of reaction synthesis on the microstructure and properties of Al_2O_3 DSC alloy were investigated, which would be helpful to provide a basis and reference for the further improvement of the process.

2 Experimental

Cu–Al alloy powders with the composition of 0.6 wt% aluminum were prepared by water atomization. The atomized powders and some oxidants were used as raw materials. After mixing, RS was performed in a gas-sealed equipment. Then the powder was hot treated in hydrogen protective atmosphere and sintered at 1,173 K for 5 min under vacuum atmosphere by "SPS-1050" spark plasma sintering (SPS) equipment. The sintering pressure and vacuum were 40 MPa and below 10 Pa, respectively. The dimension of the sample is Φ 30 mm $\times$ 5 mm.

X.-H. Zhang, C.-G. Lin*, S. Cui, Z.-D. Li
Powder Metallurgy & Special Materials Research Department, General Research Institute for Nonferrous Metals, Beijing 100088, China
e-mail: pm@grinm.com

The density of Cu–Al_2O_3 compacts was determined by using Archimedes drainage method. The theoretical density of alloy was calculated from the simple rule of mixtures, taking the full dense values for copper and Al_2O_3 were 8.96×10^3 and 2.70×10^3 kg·m^{-3}, respectively. The hardness was measured at five different positions by "HDI-1875" Rockwell hardness tester at room temperature, with its load of 98 N and loading time of 10 s. Electrical conductivity (%IACS, $IACS_{20°C} = 0.5800$ MS·m^{-2}) was tested with "SIGMA-SCOPE-LSMP" eddy current electro-conductive device. The microstructures of the Al_2O_3 DSC-sintered compacts were investigated and analyzed by means of "JSM-7001F" field emission-scanning electron microscope (FE-SEM) and its incidental energy dispersive spectrometer (EDS). Meanwhile, the morphology and distribution of Al_2O_3 particles were also observed. Nanoscale Al_2O_3 dispersoids were extracted from Al_2O_3 DSC alloys by chemical method; the phase characterizations of the powders were studied by X'Pert PRO MPD X-ray diffractometer with Cu Kα radiation.

3 Results and discussion

3.1 Microstructure and performance of Al_2O_3 DSC alloys

Cu/Al_2O_3 composites can be fabricated at 1,173 K for 5 min under vacuum environment by SPS equipment which utilized reactive synthetic Cu/Al_2O_3 powders directly without any forming process. SPS process is the most ideal one with high performance [12], and the research on SPS behavior of the alloy will be beneficial to the following material industrial production.

Figure 1 shows the microstructure of Al_2O_3 DSC alloy by SPS process. According to Fig. 1, Al_2O_3 DSC-sintered alloy has more fine structure, in which large granules with lamellar appearance are composed of small particles by agglomeration. EDS analyses show that the nanoparticles are composed of aluminum and oxygen elements, as shown in Fig. 2. Observations indicate that Al_2O_3 DSC alloy is almost densified completely with few residual micro-pores

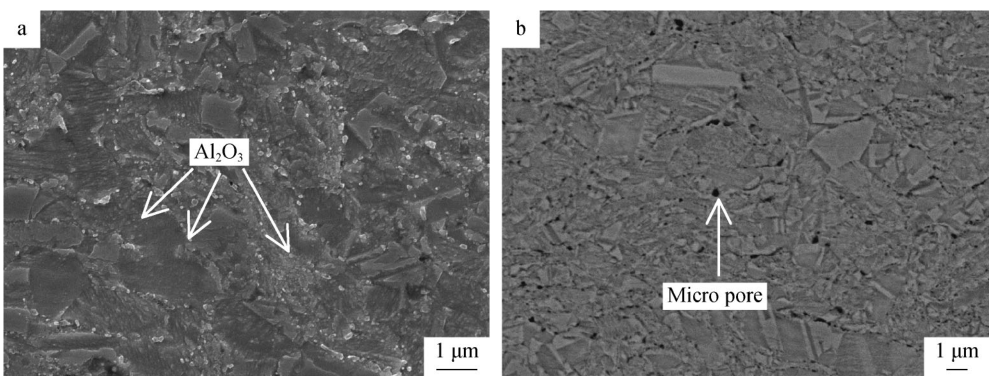

Fig. 1 SEM images of Cu–Al_2O_3 alloy by SPS of **a** secondary electron image and **b** backscattered electron image

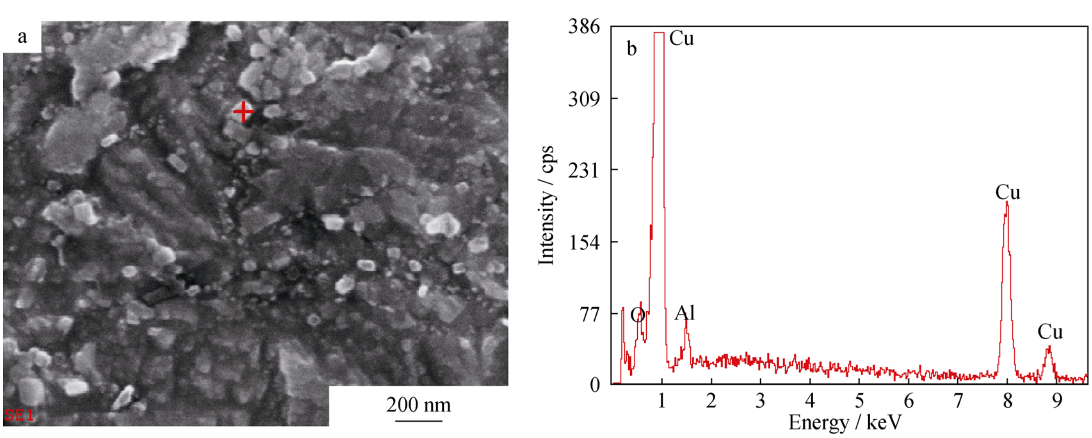

Fig. 2 SEM image and EDS analysis of Cu–Al_2O_3 alloy

in the corner between copper grains, which is consistent with the density of alloy of about 99 % T.D. tested by using Archimedes method.

The properties of SPS-sintered alloy are tested and compared with Glidcop® Al-60 alloy [13, 14], which is made by using traditional internal oxidation method. Glidcop® Al-60 alloy has the same composition with our alloy. According to Table 1, the value of electrical conductivity of SPS-sintered alloy is 72 % IACS approximate to the value of Glidcop® Al-60 alloy, while the hardness of SPS-sintered alloy is HRB 91 which is much higher than that of Glidcop® Al-60 alloy. According to Orowan strengthening mechanism [15, 16] and fine grain strengthening theory [17], tiny Al_2O_3 particles distributed uniformly in Cu matrix can hinder the motion of dislocation and improve the strength of composites material. The smaller the size of Al_2O_3 particles and the Cu grains are, the bigger the blocking effect on dislocation movement is, the strengthening effect can get more notable. Besides, a lot of nanoscale twin crystals existing inside the grains of copper are observed (Fig. 3). Dislocation prefers to plunge in front of twin crystal so as to form dislocation group pile-up, which strengthens the alloy as well.

Table 1 Properties comparison between reactive synthesis and Glidcop® Al-60 alloy

Alloy	Al composition/ wt%	Density/ (g·cm^{-3})	Electrical conductivity at 20 °C/%IACS	Rockwell hardness (HRB)
Reactive synthesis	0.6	8.76	72	91
Glidcop® Al-60	0.6	8.78	78	80

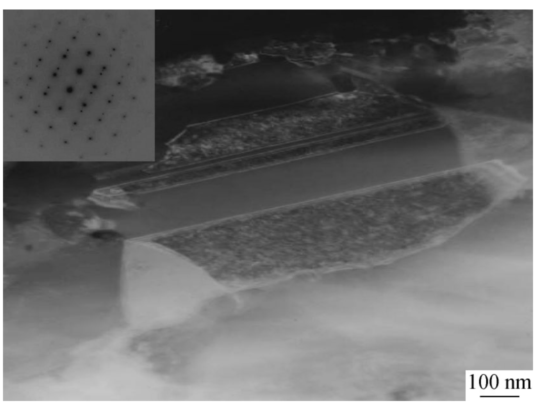

Fig. 3 Twins in DSC alloy by reactive synthesis process

3.2 X-ray diffraction (XRD) analysis

As is known to us, if all aluminum element in Cu–0.6 wt%Al alloyed powders transferred completely into alumina, the weight percent of Al_2O_3 is 1.12 wt%. Nano-sized Al_2O_3 particles with low volume fractions cannot be detected by XRD method. So it is necessary to collect these nanoparticles by extraction method. This process was carried out on the basis of relevant standard named "atomizing copper powder" (YS/T 499-200 6). Figure 4a shows the XRD pattern of the extracted dispersoids from the SPS alloy. The result reveals that the phase structure of Al_2O_3 dispersoids is only γ-Al_2O_3. A variety of crystal defects, such as dislocations, stacking faults, vacancies, and a great number of grain boundaries [18] can be formed during the RS stage. Owing to the presence of these defects, the diffusion distances decrease and the diffusibility of oxygen increases at selected temperature. Besides, the generated fresh surface of copper is beneficial to the oxygen diffusion and selective combination between aluminum and oxygen elements.

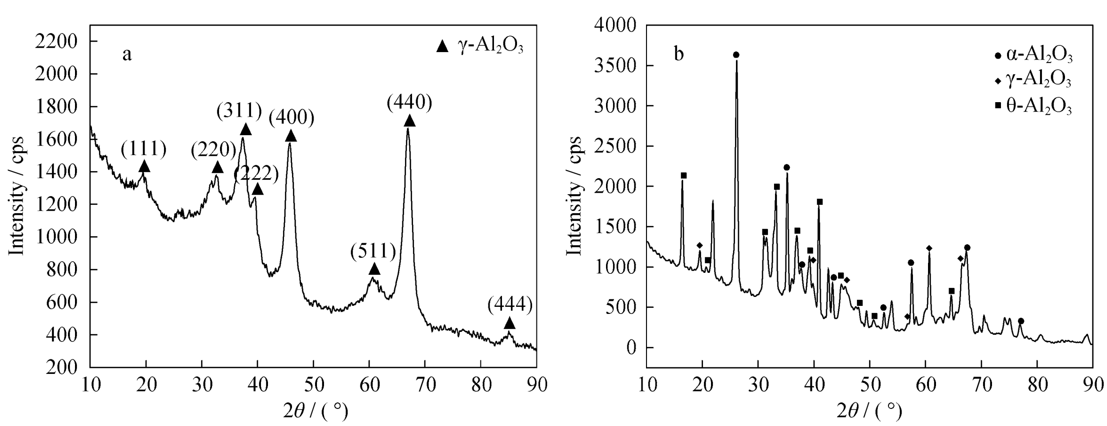

Fig. 4 XRD patterns of extracted dispersoids from DSC alloys by **a** novel reactive synthesis and **b** traditional internal oxidation

For comparison, the extracted Al_2O_3 from as-extruded DSC alloy by traditional internal oxidation method of our department was detected by XRD method [19]. The result is shown in Fig. 4b. It is demonstrated that the phase structures of Al_2O_3 are composed of α-Al_2O_3, γ-Al_2O_3, and θ-Al_2O_3. The main phase is α-Al_2O_3. According to Ref. [20], α-Al_2O_3 and θ-Al_2O_3 always exist in the grain boundary of copper, while γ-Al_2O_3 can be found inside copper grains. When nano-sized dispersoid exists in copper grains, the strength of copper is higher than that exists on grain boundary in accordance with the Orowan mechanism. It also depends on the difference of interface structure, dispersoid size, and interval. Both the crystal structure of copper and γ-Al_2O_3 are face center cubic (fcc), and the lattice parameter of copper and γ-Al_2O_3 are 0.361 and 0.395 nm, respectively, it is easy for them to form coherent interface boundary [19]. But the crystal structure of α-Al_2O_3 is rhombohedral. The lattice mismatch of α-Al_2O_3 and copper is larger than that of γ-Al_2O_3 and copper.

The values of dispersoid size figured out by using Scherer's formula are shown in Table 2. Through calculation, the size of γ-Al_2O_3 fabricated by RS/SPS process is smaller than that of three-Al_2O_3 synthesized by traditional internal oxidation process. This is an evidence to explain why the hardness of SPS-sintered copper alloy is higher.

Table 2 Comparison of phase structures and dispersoid size of Al_2O_3 DSC alloys prepared by RS/SPS or IO process

Specimen preparation method	Dispersoid phase structures	Dispersoid size/nm
Reactive synthesis and SPS	γ-Al_2O_3	27.4
Internal oxidation	α-Al_2O_3	49.4
	θ-Al_2O_3	81.0
	γ-Al_2O_3	63.3

3.3 Morphology of extracted dispersoids

Figure 5 gives the SEM images of extracted dispersoids from Al_2O_3 DSC alloy by novel RS and traditional internal oxidation process. The SEM image in Fig. 5a shows that extracted Al_2O_3 dispersoids exist in the form of nanofibers or nanofloccus, which come from nano-Al_2O_3 dispersoids agglomeration. The dimension of Al_2O_3 particles is about a few nanometers. The SEM image in Fig. 5b shows the morphology of Al_2O_3 extracted from Al_2O_3 DSC alloy by traditional internal oxidation process. The dispersoids exist in the form of powder clusters which are composed of a number of Al_2O_3 rods with its diameter of around 10 nm. This is another witness to explain why the hardness of our SPS-sintered Al_2O_3 DSC alloy is higher.

4 Conclusion

Al_2O_3 DSC alloys were successfully fabricated by a novel RS and SPS process at selected temperature. Al_2O_3 DSC-sintered alloy is almost densified completely with few residual pores between copper grains. The density is about 99 % T.D. Nano-sized Al_2O_3 dispersoids are uniformly distributed in copper matrix. The phase structure of Al_2O_3 prepared by a novel RS process is only nanometer γ-Al_2O_3, while the phases structure of Al_2O_3 are composed of α-Al_2O_3, γ-Al_2O_3, and θ-Al_2O_3 in traditional internal oxidation alloys. The crystallite size of γ-Al_2O_3 is smaller. Meanwhile, the electrical conductivity of the SPS-sintered alloy is 72 % IACS approximate to that of Glidcop® Al-60 alloy, while the Rockwell hardness can reach as high as HRB 91.

It is noteworthy that the reason of twin crystals formation and its effects on DSC alloy is not clearly; the interface between Al_2O_3 particles and copper matrix should be observed. These will be topics in our future research work.

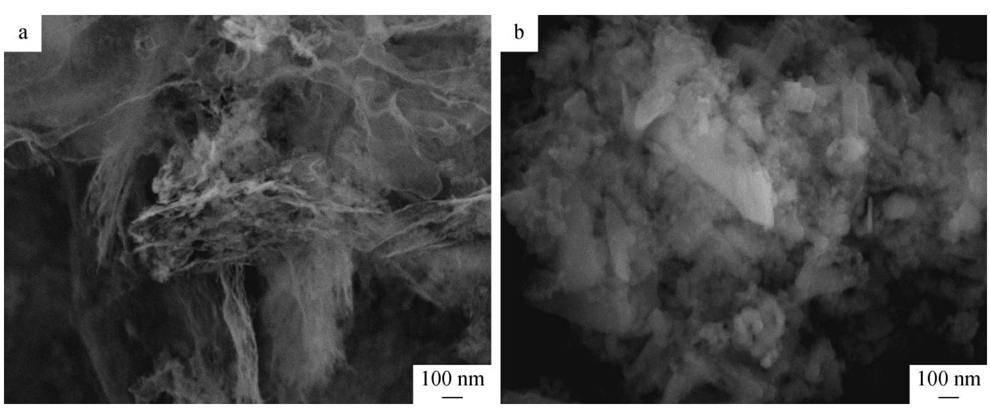

Fig. 5 SEM image of extracted dispersoids from DSC alloys by **a** RS/SPS and **b** traditional IO process

Acknowledgments This work was financially supported by the National Natural Science Foundation of China (No. 5043202). Authors are grateful to Dr. Peng Yan, Mr. Xue-Wen Liu, and Mr. Xiao-Kang Hu for their assistance in the experimental work.

References

[1] Jena PK, Brocchi EA, Solórzano IG, Motta MS. Identification of a third phase in Cu–Al_2O_3 nano-composites prepared by chemical routes. Mater Sci Eng A. 2004;371(1–2):72.

[2] Shehata F, Fathy A, Abdelhameed M, Moustafa SF. Prepartion and properties of Al_2O_3 nanoparticle reinforced copper matrix composites by in situ processing. Mater Des. 2009;30:2756.

[3] Stobrawa JP, Rdzawski ZM. Dispersion-strengthened nano-crystalline copper. J Achiev Mater Manuf Eng. 2007;24(2):35.

[4] Krawczyk FL, Bolme GO, Clark WL. Rf-loss measurements in an open coaxial resonator for characterization of copper plating. In: Proceedings of PAC07 Committee. New Mexico; 2007. 2376.

[5] Ding J, Zhao N, Shi C, Li J. In situ formation of Cu-ZrO_2 composites by chemical routes. J Alloy Compd. 2006;425(1–2):391.

[6] Motta MS, Jena PK, Brocchi EA. Characterization of Cu–Al_2O_3 nano-scale composites synthesized by in situ reduction. Mater Sci Eng C. 2001;15(1):175.

[7] Li G, Sun J, Guo Q. Fabrication of the nanometer Al_2O_3/Cu composite by internal oxidation. J Mater Process Technol. 2005; 170(1):336.

[8] Benjamin JS. Dispersion strengthened superalloys by mechanical alloying. Met Trans. 1970;8(1):2943.

[9] Li Z, Shen J, Cao F, Li Q. A high strength and high conductivity copper alloy prepared by spray forming. J Mater Process Technol. 2003;137(1–3):60.

[10] Rodrigo HP, Aquiles S, Rodrigo E. High-temperature deformation of dispersion-strengthened Cu–Zr–Ti–C alloys. Mater Sci Eng A. 2005;391(1–2):60.

[11] Rodrigo AE, Rodrigo HP, Aquiles OS. Micro- structural characterization of dispersion strengthened Cu–Ti–Al alloys obtained by reaction milling. Mat Sci Eng A. 2007;454–455:183.

[12] Dash K, Ray BC, Chaira D. Synthesis and characteristics of copper–alumina metal matrix composite by conventional and spark plasma sintering. J Alloy Compd. 2012;516(7):78.

[13] Mehrabian R, Flemings MC. Metal composition and methods for preparing liquid–soild alloy metal compositions and for casting the metal compositions. US Patent 3951651, 1976.

[14] Li M, Guo Z, Zhao Q. Progress in and applications of copper-based alloys. Powder Metall Ind. 2008;18(1):36.

[15] Kudashov DV, Baum H, Martin U, Heilmaier M, Oettel H. Microstructure and room temperature hardening of ultra-fine-grained oxide-dispersion strengthened copper prepared by cryomilling. Mater Sci Eng A. 2004;387–389(4):770.

[16] Palma HR, Sepulveda OA. Contamination effects on precipitation hardening of Cu–alumina alloys prepared by mechanical alloying. Mater Sci Forum. 2003;416–418(98):164.

[17] Ďurišinová K, Ďurišin J, Orolínová M. Al_2O_3-dispersion strengthened nanocrystalline copper. Powder Metall Prog. 2006; 6(2):77.

[18] Huang J, Wu Y, Ye H. Microstructure investigations of ball milled materials. Microsc Res Tech. 1998;40(2):116.

[19] Lu Y, Cui S, Kang Z, Zhou W. Microstructure and precipitation process of dispersoids of dispersion strengthened copper alloy. Mater Rev. 2006;20(Sl):220.

[20] Yan P, Lin C, Cui S, Lu Y, Zhou Z, Li Z. Microstructural features and properties of high-hardness and heat-resistant dispersion strengthened copper by reaction milling. J Wuhan Univ Technol Mater Sci Ed. 2011;26(5):905.